Influence of scale effects on local stiffness of filled elastomers in structural modeling

Ilya A. Morozov Bernd Lauke
ilya.morozov@gmail.com

Abstract

A realistic model of spatial arrangement of fillers in rubber is developed. Structural parameters of the model as the distribution of filler size, characteristics of secondary clusters and the presence of large bulk particles (micropellets) are taken from AFM-scans of carbon black filled rubber vulcanizates. A descriptor of filler distribution in the matrix - inhomogeneity index is suggested. The analysis of stiffness and inhomogeneity index of synthesized 3D-structures allowed to judge the reliability of different simplifications, as fillers of the same size or random filler arrangement and the absence of micropellets in structural modelling. Investigation of stiffness versus the size of modelled volumes showed large deviations of measured values at small scale of observation ($\approx 1\mu m$).

1 Introduction

The addition of active fillers (carbon black, silanized silica) to a rubber matrix leads to significant reinforcement of composites. This reinforcement is manifested as an increase in the toughness, durability of elastomers and, consequently to a longer service life, whereas their elasticity and ability to multiple reversible deformations caused by stretching remain unchanged. This is mainly due to strong interphase physicochemical interactions proceeding in the composite. Filled elastomers are heterogeneous materials and have a microstructure consisting of spatially connected clusters. A continuous filler network formed in the material by the branches of fractal clusters even at a relatively low filler volume fraction of $\approx 12\%$.

To predict the macroscopic response of such composites under external loading, the model should reflect in full measure the peculiarities of the microstructure of materials and demonstrate the interactions between neighbor components. The high processing capabilities of modern computers make it possible to directly model a representative volume of the filler network and then to apply some external loading. A starting point for such simulations must be information about filler geometry and arrangement in the polymer matrix. The new methods of analysis of AFM-images of filled rubbers developed recently [1] allowed us to determine the filler geometry and parameters of secondary clusters. This paper focuses on a method for computer synthesis of spatial filler networks. Input parameters for the model are taken from the structural analysis of AFM-images of filled rubbers.

To investigate the changes of stiffness, such variables as filler fraction, size of representative volume, presence or absence of single large inclusions, random or cluster filler arrangement, and filler size (filler particles are equal in size, or particles sizes are distributed in a log-normal fashion) are taken into account. Much attention is paid to the estimation

of a minimal reliable size of the structure (mesoscale) to ensure that consideration is given to a typical representative volume element.

2 Experiments and data analysis

In order to obtain input parameters for the model, carbon black filled styrene-butadiene vulcanizate samples were examined. The content of carbon black of 10, 30 and 50 phr (i.e., grams of carbon black per 100 grams of polymer) corresponds to the volume fractions of 0.04, 0.13 and 0.21, respectively.

Experiments were carried out on an atomic force microscope Bruker Icon. The surfaces of fresh cuts of filled polymer samples were examined. To perform statistical data analysis, a few high-quality scans were acquired for each material and further analyzed using our algorithms developed in Matlab. Example of microstructure image and processing results are presented in Fig. 1.

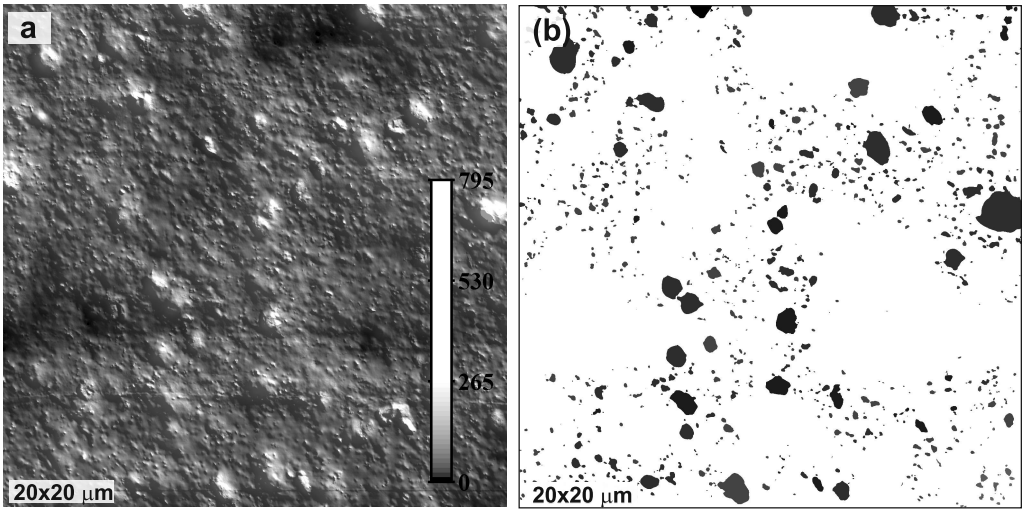

Figure 1: AFM-image of the surface of SBR/50 (a) and the result of image segmentation (b)

The algorithm of image segmentetion involves two steps. 1): Find any local maxima of the surface under study (vertices of future segments). 2): Examine the contour lines around the obtained maxima and determine the boundaries of segments. Hence, the continuous relief is divided into separate field of segments.

Examination of the sizes and shapes of segments allowed us to define two types of inclusions in the polymer: 1) micropellets - for segments of size $\geq$ 300 nm and compactness $\geq$ 0.85. 2) filler aggregates - for the rest of segments. The fraction of micropellets is calculated as the ratio of the total area of the bases of micropellets to the total area of filler fragments. The results show that the fraction of micropellets decreases with increasing filler concentration: 41, 23 and 1.1% for SBR/10, 30 and 50 phr respectively. The average size of such structures is 555, 457, 354 nm. The aggregate size distributions in the materials under study can be fairly well approximated by the log-normal probability distribution density law with known parameters.

The segmented surfaces are not homogeneous. It is seen that these surfaces have the high filler concentration regions connected by branches, i.e., the visible parts of spatial secondary structures (agglomerates). The number of primary structures (aggregates), N, is related to the size of agglomerates, R by the fractal distribution law as $N = \mu R^D$,

where μ is the constant, and D is the fractal dimension. The algorithms for image analysis developed previously [1] allowed us to calculate the fractal dimensions of the secondary structures of filler aggregates in the materials under study: 1.78 for SBR/30 and 2.02 for SBR/50. The number of secondary structures per $1\mu m^2$ of image is 0.06 and 0.11 respectively (name this parameter α).

To quantify the filler distribution (non-spherical objects of different sizes) in the observed areas, the heterogeneity index, J, is introduced. This value indicates the minimum size of the window, where the filler arrangement is assumed to be homogeneous and can be calculated as: the m squares of size s^2 are randomly chosen in the examined image, and $J(s)$ is defined as

$$J(s) = (min(A_i/s^2) + max(A_i/s^2))/(2\varphi^*)$$

where A_i is the area occupied by filler segments in the i-th square; φ^* - total fraction of area occupied by segments in the analyzed image. The number of squares, m, is obtained using the following equation: $m = 0.1exp(-7s/L)$. The closer the value of $J(s)$ to unity, the more homogeneous the distribution of the filler throughout the material will be at this scale. With decreasing s, the window starts to get the areas of both the high and low filler concentration. The value of s^*, from which $J(s)$ substantially deviates from unity, can be regarded as a critical scale (mesoscopic scale); for any scale $s \geq s^*$, the filler distribution can be considered as homogeneous. For the examined materials s^* is 13, 8 and 5 μm.

3 Structural model of filled rubber

The structure is modeled by a cube of side-length H. The cube is filled with spheres representing micropellets or aggregates. The side H is related to the mesoscopic scale as $H = 1.5s^*$. To avoid boundary effects, the cube of a greater volume was constructed, and all the statistics were calculated in its central part with side-length s^*. The sizes of spheres-micropellets were generated using uniform random distribution until the given fraction of micropellets was reached. After that, they were arbitrarily placed in inside the volume H^3. The aggregates were generated using the lognormal distribution of sizes until the total filler fraction was obtained. To construct the spatial network of secondary structures, the cores of agglomerates were randomly placed in the volume. The number of cores is related to the parameter α as $(\alpha H^2 + 1)^3$. The fractal agglomerates of dimension D grew sequentially around the cores until all the spheres were placed in the volume. The algorithm to connect the i-th sphere and the k-agglomerate is as follows.

Let R_k be the size of the k-th agglomerate. The initial R_k is equal to the radius of agglomerate core. The numbers of spheres belonging to this agglomerate and located at a distance $\leq R_k \pm R_\delta$ from its core are collected into an array $\{a\}$, where R_δ is supposed to be the average diameter of aggregates. An arbitrary value a_j is taken from the array $\{a\}$. Next, a series of trials are made to place the i-th sphere near the a_j-th sphere avoiding the intersections of the i-th sphere and the existing structures. To do this, the coordinates of the i-th sphere are set using the randomly chosen spherical angles with respect to the a_j-th sphere. If all the trials fail, then the next arbitrary sphere with the number from the array $\{a\}$ is taken (previous a_j-s are not considered). If all the elements from the array $\{a\}$ are checked and the i-th sphere is not yet connected with the k-th agglomerate this means that the k-th agglomerate has reached its maximum size. In this case, further growth of this agglomerate is stopped, and the i-th sphere is placed into the arbitrary unoccupied region of the volume and becomes the core of a new agglomerate. In the case of successful dislocation of the i-th sphere in the k-th agglomerate, the analysis of the

fractal dependence between the existing number of spheres N_k and its size is performed. if $N_k > R_k^D$ then the agglomerate size increases: $R_k = R_k + R_\delta$.

After all of this is over, the next $i+1$ sphere-aggregate is connected with the $k+1$ agglomerate (or the first agglomerate, if the last has been reached), until all the spheres are placed inside the volume.

As regards the minimum distance between the aggregates (spheres) in the model, it is impossible to extract it from the AFM-images because of the limitations associated with the AFM-tip dimensions (10 nm). However, according to the dielectric spectroscopy measurements [2], the minimal distance between the carbon black aggregates is ranging between 2 and 5 nm.

4 Results and discussion

Apart from the structures synthesized using all the above mentioned parameters (case I), the simplified realizations of these structures are constructed: case II - without micropellets; case III - without micropellets and with spheres of equal size; case IV - without micropellets, with spheres of equal size and with random filler arrangement in the matrix. Since the size s^* is quite high, the constructed volumes look like black cubes. For better representation, only the "cuts" of the obtained materials - the spheres, whose z-coordinates are within 500 nm from the centre of the volume - are shown in Fig. 2.

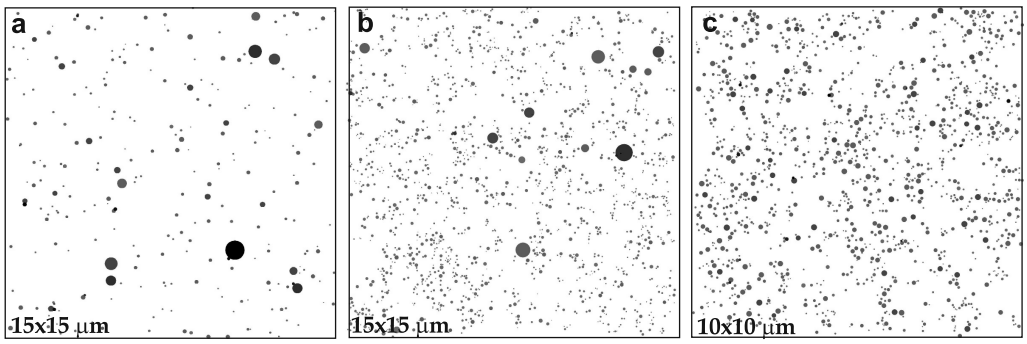

Figure 2: 'Cuts' of the obtained structures - SBR/10 (a), SBR/30 (b), SBR/50 (c).

For comparison of the synthesized structures with their simplified versions from the viewpoint of their mechanical stiffness and the development of the continuous filler-network, the gap l_{gap} between the closest spheres comprising the sample chain from top to bottom was measured. That is, the first sphere at the top is arbitrarily selected, the closest sphere that lies lower is found, the in-between gap is measured, the next lower sphere closest to the second is found, and so on until the bottom is reached. The condition 'the closest sphere that lies lower' means that the z_i-coordinate of the centre of the i-th sphere which is closest to the k-th sphere must lie lower than the point $z_k - R_k$.

In the case of small extension applied to the modelled volume, the mechanical response of the domain in the gap between the adjacent spheres can be described as the stiffness, G, of an elastic rod. This type of modelling [3] provides the following relationship between the gap size and stiffness:

$$G = E_m R_{min}^2 (25 + 4\psi) ln(1+\psi) (\delta / R_{min})^{0.15 ln(\delta/R_{min}) - 0.2 ln(0.5+\psi)}$$

where E_m is the elastic modulus of the material in the gap; δ is the gap between the spheres with radii R_{max} and R_{min}, calculated in the same way as l_{gap}; $\psi = R_{max}/R_{min}$

The values of the gap between the spheres and the average force F_z ($F_z = G_u$) in the chain going from top to bottom are summarized (for extension $u = 1$ nm and modulus E_m 1 MPa) in Table 1. The table does not include any data for the materials with 10 phr because at low filler concentration no branchy structures of agglomerates appear.

	SBR/30				SBR/50			
	I	II	III	IV	I	II	III	IV
gap l_g, nm	29.8	27.3	19.3	42.2	22.1	22.6	13.6	13.4
Fz, kN	77	75	42	23	75	76	30	16.1

Table 3: Comparison of different realizations of the structure

I - 'actual' structure; II - without micropellets; III - without micropellets, spheres of equal size; IV - without micropellets, spheres of equal size, random filler distribution.

As shown in Table, in all cases there are differences between the 'actual' and simplified structures: a) the absence of micropellets (large-size inclusions) results in a minor decrease in the gap, and thus the stiffness of the system changes; b) the spheres of equal size provide a significant (20-30%) decrease in the gap size, as well as in the stiffness; c). Random filler distribution causes a three-fold reduction in stiffness and a slight increase in the gap size (significant for SBR/30).

Index of inhomogeneity J_3 for the spatial structures could be calculated by simply changing areas to volumes in eq. (1). However, this drastically increases the calculation time. Thus, $J_3(s)$ was approximated with average value in the cross-sections of the 'sample'. Results are shown in Fig. 3.

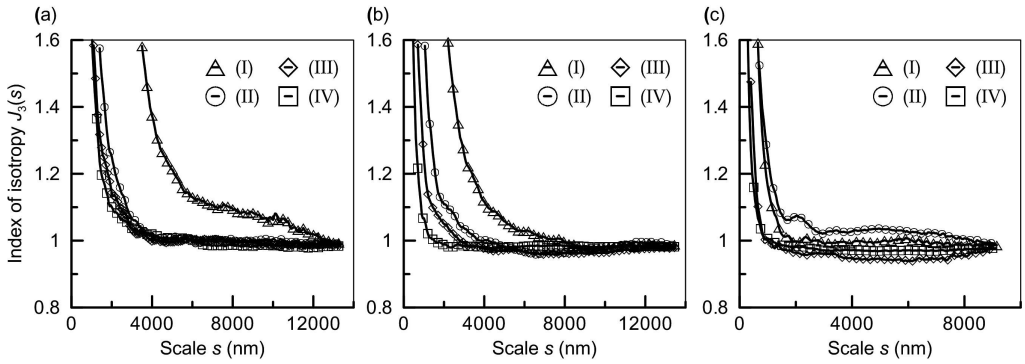

Figure 3: Heterogeneity index for different realizations of spatial structures: (a) - SBR/10, (b) - SBR/30, (c) - SBR/50.

The value of the scale factor, s, at which J(s) falls to almost unity, gives the minimum size at which the material can be considered as a homogeneous one. Absence of micropellets (II), usage of spheres of same size (III) and random filler distribution (IV) decrease the inhomogeneities of filler distribution, especially for the materials with 10 and 30 phr (Fig. 3). The results clearly show that the presence of large inclusions in the material sufficiently changes the homogeneity of the composite. At the same time, the presence of micropellets changes only slightly the stiffness and gap size of volumes filled with spheres (See Table). Thus, if one intends to use such systems to model the mechanical response of filled rubbers, the micropellets can be neglected, but the other structural properties should be taken into account. For case (I), the mesoscale is equal to 2000 nm for SBR/50, 6000 nm for SBR/30 and 11000 nm for SBR/10, respectively. For case (II), the mesoscale is equal to 2000 nm SBR/50, 3500 nm for SBR/30 and 4000 nm SBR/10, respectively.

Consider how the choice of a representative size of the volume influences the stiffness of the 'sample'. To this end, a number of volumes with a variable side length, s, were cut arbitrarily from different places of large structures, and the average value of F_z and the standard deviation were computed (Fig. 4).

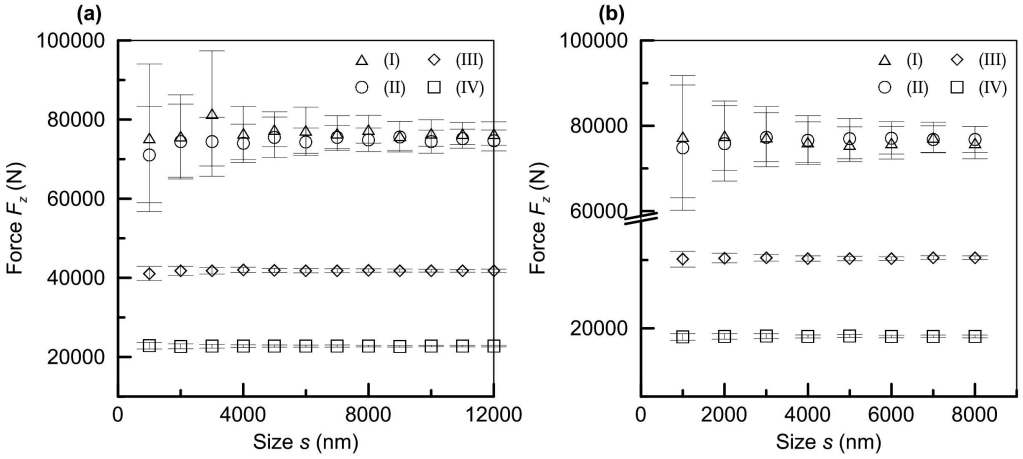

Figure 4: Tensile force of the "sample" versus its size for SBR/30 (a) and SBR/50 (b).

The vertical bars in Figure 4 mark standard deviation. It is shown that the significant variation of stiffness (force) is observed for small representative volumes (Fig. 4a). This fact once again points out that the structural-mechanical investigation of such structures based on the relatively small volumes can lead to essential disagreement with the bulk properties. It is clearly shown that the standard deviation approaches some asymptotic value as the variable side length, s, increases. These values of s are in agreement with study when $J(s)$ goes down to unity (see Fig. 3). The absence of micropellets (case II) and other simplifications of the model also decrease the deviation and reduce the path to asymptote.

5 Conclusion

An algorithm has been developed to construct the spatial structures reflecting the peculiarities of the actual microstructure of filled polymers. The following structural properties have been considered: the arrangement of filler particles in secondary structures (agglomerates), the minimum representative size of the modelled volume, the lognormal aggregate size distribution, and the presence of large particles. These input parameters of the model were determined in the structural analysis of the AFM-images of the materials under study. To evaluate the size of filler dispersion inhomogeneity, a new characteristic - the heterogeneity index - was introduced. To find the input parameters for the model, the structural analysis of styrene-butadiene carbon black filled vulcanizates with 10, 30 and 50 mass parts of filler was performed. The simulation results reveal that the presence of micropellets increases the scale of inhomogeneity of filler dispersion, but changes the stiffness of the materials only slightly. It is shown that the use of 'fillers' of equal size increases the homogeneity of the structure but decreases its stiffness. All the observed effects are more pronounced at low and moderate filler concentrations. The approach and results presented here will be used further in structural-mechanical modelling of filled elastomers.

Acknowledgements

The work was supported by the grant of the President of the Russian Federation (MK-3914.2011.8) and the RFBR-grant (11-08-00178-a).

References

[1] Morozov I.A., Lauke B., Heinrich G. A New approach to quantitative microstructural investigation of carbon black filled rubbers by AFM // Rubber chemistry and technology. 2012. (in print).

[2] J. G. Meier, M. Kluppel. Carbon Black Networking in Elastomers Monitored by Dynamic Mechanical and Dielectric Spectroscopy // Macromolecular materials and engineering. 2008. V. 293. P. 12-38.

[3] Moshev V.V., Garishin O.K. Physical discretization approach to evaluation of elastic moduli of highly filled granular composites // International Journal of Solids and Structures. 1993. V. 30. No. 17. P. 2347-2355.

Ilya A. Morozov, str. Koroleva 1,Perm, Russia
Bernd Lauke, Hohe str. 6, Dresden, Germany